

# Crystal structure of 2-oxo-2*H*-chromen-3-yl 4-chlorobenzoate and Hirshfeld surface analysis

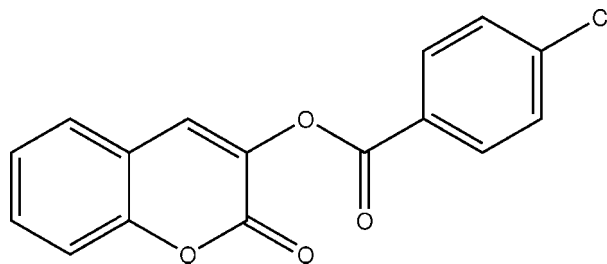
Eric Ziki,<sup>a\*</sup> Siaka Sosso,<sup>b</sup> Frédérica Mansilla-Koblavi,<sup>a</sup> Abdoulaye Djandé<sup>b</sup> and Rita Kakou-Yao<sup>a</sup>

<sup>a</sup>Laboratoire de Cristallographie et Physique Moléculaire, UFR SSMT, Université Félix Houphouët Boigny de Cocody 22 BP 582 Abidjan 22, Côte d'Ivoire, and <sup>b</sup>Laboratoire de Chimie Moléculaire et Matériaux, Equipe de Chimie Organique et Phytochimie, Université Ouaga 1 Pr Joseph KI-ZERBO 03 BP 7021 Ouagadougou 03, Burkina Faso. \*Correspondence e-mail: eric.ziki@gmail.com

In the title compound, C<sub>16</sub>H<sub>9</sub>ClO<sub>4</sub> the dihedral angle between the coumarin ring system [maximum deviation = 0.023 (1) Å] and the benzene ring is 73.95 (8)°. In the crystal,  $\pi$ - $\pi$  interactions link the dimers into a three-dimensional framework. A quantum chemical calculation is in generally good agreement with the observed structure, although the calculated dihedral angle between the ring systems (85.7%) is somewhat larger than the observed value [73.95 (8)°]. Hirshfeld surface analysis has been used to confirm and quantify the supramolecular interactions.

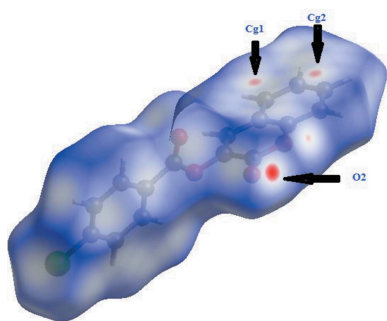
## 1. Chemical context

Coumarin and its derivatives are widely recognized for their multiple biological activities, including anticancer (Lacy *et al.*, 2004; Kostova, 2005), anti-inflammatory (Todeschini *et al.*, 1998), antiviral (Borges *et al.*, 2005), anti-malarial (Agarwal *et al.*, 2005) and anticoagulant (Maurer *et al.*, 1998) properties. As part of our studies in this area, we now describe the synthesis and crystal structure of the title compound, (I).



## 2. Structural commentary

In compound (I) (Fig. 1), the coumarin ring system is, as expected, almost planar [maximum deviation = 0.023 (1) Å] and is oriented at an angle of 73.95 (8)° with respect to the benzene ring. An inspection of the bond lengths shows that there is a slight asymmetry of the electronic distribution around the coumarin ring: the C3—C2 [1.335 (2) Å] and C2—C1 [1.456 (2) Å] bond lengths are shorter and longer, respectively, than those expected for a C<sub>ar</sub>—C<sub>ar</sub> bond. This suggests that the electronic density is preferentially located in the C2—C3 bond at the pyrone ring, as seen in other coumarin derivatives (Gomes *et al.*, 2016; Ziki *et al.*, 2016).



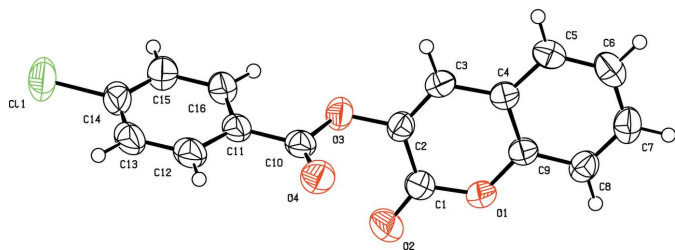


**Figure 1**  
The molecular structure of compound (I), with displacement ellipsoids drawn at the 50% probability level.

### 3. Supramolecular features

In the crystal, weak aromatic  $\pi$ - $\pi$  stacking interactions (Janiak, 2000) are present [ $Cg1 \cdots Cg2(1-x, -y, 1-z) = 3.4781(10) \text{ \AA}$  and  $Cg2 \cdots Cg2(1-x, 1-y, 1-z) = 3.5644(11) \text{ \AA}$ , where  $Cg1$  is the centroid of the coumarin pyran ring and  $Cg2$  is the centroid of the coumarin benzene ring], thus forming a three-dimensional supramolecular network. A weak  $C11=O4 \cdots Cg3(1-x, -y, -z)$  ( $\pi$ -ring) interaction between  $O4$  and a symmetry-related benzene ring ( $C6$ - $C11$ , centroid  $Cg3$ ) of is also present (Fig. 2).

### 4. Hirshfeld surface analysis

*Crystal Explorer3.1* (Wolff *et al.*, 2012) was used to generate the Hirshfeld surface and two-dimensional fingerprint (FP) plots (Rohl *et al.*, 2008). The analysis of intramolecular and intermolecular interactions through the mapping of  $d_{\text{norm}}$  is permitted by the contact distances  $d_i$  and  $d_e$  from the Hirshfeld surface to the nearest atom inside and outside, respectively. In compound (I), there are four O atoms and a Cl atom that can potentially act as acceptors for hydrogen bonds, but one of O

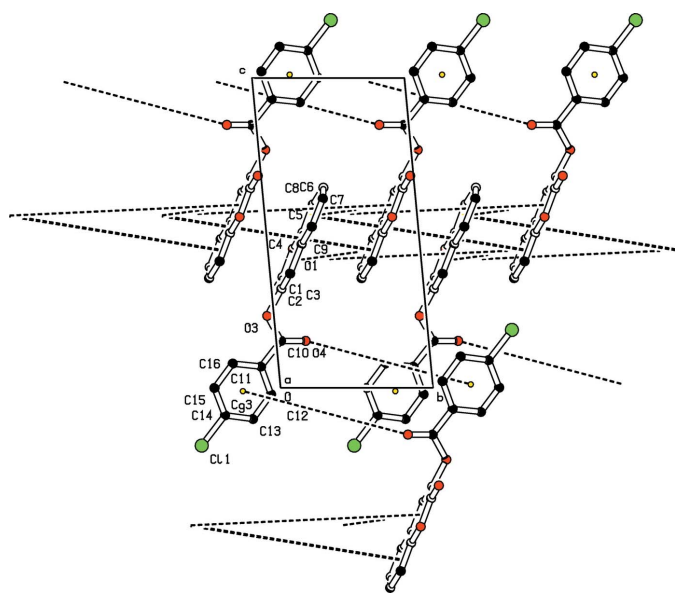


**Figure 2**  
Partial packing diagram for (I), showing the  $\pi$ - $\pi$  stacking and  $C-O \cdots \pi$  interactions (dashed lines). The yellow dots are ring centroids. H atoms have been omitted for clarity.

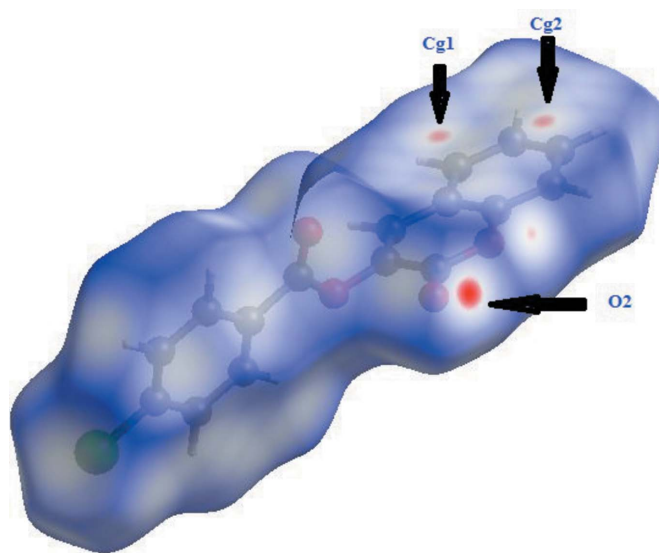


**Figure 3**  
A view of the Hirshfeld surface mapped over  $d_{\text{norm}}$ . The contact points (red) are labelled to indicate the atoms participating in the intermolecular interactions.

atoms and the H atom of the chlorobenzoate moiety are involved in the establishment of intramolecular hydrogen bonds. The surface mapped over  $d_{\text{norm}}$  displays four red spots that correspond to areas of close contact between the surface and the neighbouring environment and is shown in Fig. 3. The contributions from different contacts were selected by partial analysis of the FP plots (Fig. 4).  $C \cdots C$  contacts correspond to intermolecular  $\pi$ - $\pi$  interactions.

The greatest contribution (26.5%) is from the  $H \cdots O/O \cdots H$  contacts, which appear as the highlighted red spot on the side of the surface (Figs. 3 and 4c). The red spots in the middle of the surface correspond to  $C \cdots C$  contacts appearing near  $d_e = d_i \simeq 1.7$  and  $1.8 \text{ \AA}$  (Fig. 4d). As expected in organic compounds, the  $H \cdots H$  contacts are important with a 24.7% contribution to Hirshfeld surface (Fig. 4b). There are also

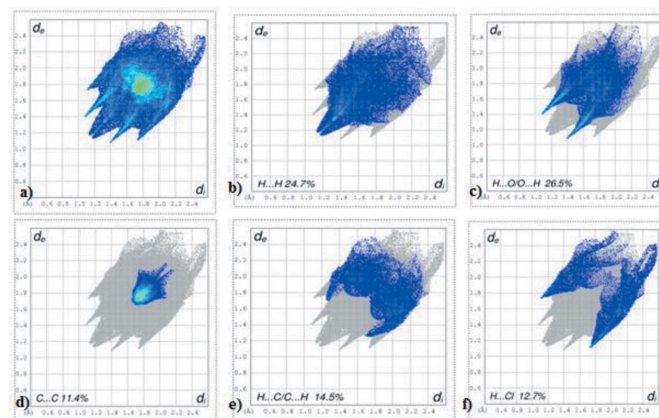


**Figure 4**  
Two-dimensional fingerprint plots: (a) overall, and delineated into contributions from different contacts: (b)  $H \cdots H$ , (c)  $H \cdots O/O \cdots H$ , (d)  $C \cdots C$ , (e)  $H \cdots C/C \cdots H$  and (f)  $H \cdots Cl/Cl \cdots H$ .

H...C/C...H and H...Cl/Cl...H contacts, which make contributions of 14.5 and 12.7%, respectively (Figs. 4e and 4f).

## 5. Quantum-chemical calculations

Quantum-chemical calculations were performed and the results compared with the experimental analysis. An *ab-initio* Hartree–Fock (HF) method was used with the standard 6-31G basis set using the *GAUSSIAN03* software package (Frisch *et al.*, 2004; Dennington *et al.*, 2007) to obtain the optimized molecular structure. The computational results are in good agreement with the experimental crystallographic data (see Supplementary Tables S1 and S2). The dihedral angle between the coumarin ring and the chlorobenzoate ring for the calculated structure is 85.7°, which is larger than the value of 73.95 (8)° for the observed structure.

## 6. Synthesis and crystallization

To a solution of 4-chlorobenzoyl chloride ( $6.17 \times 10^{-3}$  mol  $\approx$  0.8 ml) in dry tetrahydrofuran (31 ml) was introduced dried triethylamine (3 molar equivalents  $\approx$  2.6 ml). While stirring strongly,  $6.17 \times 10^{-3}$  mol (1 g) of chroman-2,3-dione was added in small portions over 30 min. The reaction mixture was then refluxed for 4 h and poured into a separating funnel containing 40 ml of chloroform. The solution was acidified with dilute hydrochloric acid until the pH was 2–3. The organic layer was extracted, washed with water until neutral, dried over MgSO<sub>4</sub> and the solvent removed. The resulting precipitate (crude product) was filtered off with suction, washed with petroleum ether and dissolved in a minimum of dichloromethane by heating under agitation. Hexane was added to this hot mixture until the formation of a new precipitate started, which dissolved in the resulting mixture upon heating. Upon cooling, yellow crystals of the title compound precipitated in a yield of 70%; m.p. 478–482 K.

## 7. Refinement details

Crystal data, data collection and structure refinement details are summarized in Table 1. H atoms were placed in calculated positions (C–H = 0.93 Å) and refined using a riding-model approximation with  $U_{\text{iso}}(\text{H}) = 1.2U_{\text{eq}}(\text{C})$ .

## Acknowledgements

The authors thank the Spectropole Service of the faculty of Sciences (Aix-Marseille, France) for the use of the diffractometer.

## References

Agarwal, A., Srivastava, K., Puri, S. K. & Chauhan, P. M. S. (2005). *Bioorg. Med. Chem.* **13**, 4645–4650.

**Table 1**  
Experimental details.

Crystal data	
Chemical formula	C <sub>16</sub> H <sub>9</sub> ClO <sub>4</sub>
<i>M<sub>r</sub></i>	300.68
Crystal system, space group	Triclinic, <i>P</i> $\bar{1}$
Temperature (K)	293
<i>a</i> , <i>b</i> , <i>c</i> (Å)	6.7866 (4), 7.1789 (3), 14.0981 (5)
$\alpha$ , $\beta$ , $\gamma$ (°)	94.098 (3), 93.461 (4), 106.154 (4)
<i>V</i> (Å <sup>3</sup> )	655.75 (5)
<i>Z</i>	2
Radiation type	Cu K $\alpha$
$\mu$ (mm <sup>-1</sup> )	2.72
Crystal size (mm)	0.12 $\times$ 0.12 $\times$ 0.08
Data collection	
Diffractometer	Agilent SuperNova Dual Source diffractometer with an Atlas detector
Absorption correction	Multi-scan ( <i>CrysAlis PRO</i> ; Agilent, 2014)
<i>T</i> <sub>min</sub> , <i>T</i> <sub>max</sub>	0.737, 0.812
No. of measured, independent and observed [ <i>I</i> > 2 $\sigma$ ( <i>I</i> )] reflections	7634, 2409, 2109
<i>R</i> <sub>int</sub>	0.022
( <i>sin</i> $\theta$ / $\lambda$ ) <sub>max</sub> (Å <sup>-1</sup> )	0.606
Refinement	
<i>R</i> [ <i>F</i> <sup>2</sup> > 2 $\sigma$ ( <i>F</i> <sup>2</sup> )], <i>wR</i> ( <i>F</i> <sup>2</sup> ), <i>S</i>	0.039, 0.106, 1.05
No. of reflections	2409
No. of parameters	190
H-atom treatment	H-atom parameters constrained
$\Delta\rho_{\text{max}}$ , $\Delta\rho_{\text{min}}$ (e Å <sup>-3</sup> )	0.26, -0.49

Computer programs: *CrysAlis PRO* (Agilent, 2014), *SHELXS97* (Sheldrick, 2008), *SHELXL2013* (Sheldrick, 2015), *PLATON* (Spek, 2009) and *pubCIF* (Westrip, 2010).

- Agilent. (2014). *CrysAlis PRO*. Agilent Technologies Ltd, Yarnton, England.
- Borges, F., Roleira, F., Milhazes, N., Santana, L. & Uriarte, E. (2005). *Curr. Med. Chem.* **12**, 887–916.
- Dennington, R., Keith, T. & Millam, J. (2007). *GAUSSVIEW4.1*. Semichem Inc., Shawnee Mission, KS, USA.
- Frisch, M. J., *et al.* (2004). *GAUSSIAN03*. Gaussian Inc., Wallingford, CT, USA.
- Gomes, L. R., Low, J. N., Fonseca, A., Matos, M. J. & Borges, F. (2016). *Acta Cryst. E* **72**, 926–932.
- Janiak, C. (2000). *J. Chem. Soc. Dalton Trans.* pp. 3885–3889.
- Kostova, I. (2005). *Curr. Med. Chem. Anti-Cancer Agents*, **5**, 29–46.
- Lacy, A. & O’Kennedy, R. (2004). *Curr. Pharm. Des.* **10**, 3797–3811.
- Maurer, H. H. & Arlt, J. W. (1998). *J. Chromatogr. B Biomed. Sci. Appl.* **714**, 181–195.
- Rohl, A. L., Moret, M., Kaminsky, W., Claborn, K., McKinnon, J. J. & Kahr, B. (2008). *Cryst. Growth Des.* **8**, 4517–4525.
- Sheldrick, G. M. (2008). *Acta Cryst. A* **64**, 112–122.
- Sheldrick, G. M. (2015). *Acta Cryst. C* **71**, 3–8.
- Spek, A. L. (2009). *Acta Cryst. D* **65**, 148–155.
- Todeschini, A. R., de Miranda, A. L. P., da Silva, K. C. M., Parrini, S. C. & Barreiro, E. J. (1998). *Eur. J. Med. Chem.* **33**, 189–199.
- Westrip, S. P. (2010). *J. Appl. Cryst.* **43**, 920–925.
- Wolff, S. K., Grimwood, D. J., McKinnon, J. J., Turner, M. J., Jayatilaka, D. & Spackman, M. A. (2012). *Crystal Explorer*. The University of Western Australia.
- Ziki, E., Yoda, J., Djandé, A., Saba, A. & Kakou-Yao, R. (2016). *Acta Cryst. E* **72**, 1562–1564.

## supporting information

*Acta Cryst.* (2017). E73, 45-47 [https://doi.org/10.1107/S2056989016019538]

## Crystal structure of 2-oxo-2*H*-chromen-3-yl 4-chlorobenzoate and Hirshfeld surface analysis

Eric Ziki, Siaka Sosso, Frédérica Mansilla-Koblavi, Abdoulaye Djandé and Rita Kakou-Yao

### Computing details

Data collection: *CrysAlis PRO* (Agilent, 2014); cell refinement: *CrysAlis PRO* (Agilent, 2014); data reduction: *CrysAlis PRO* (Agilent, 2014); program(s) used to solve structure: *SHELXS97* (Sheldrick, 2008); program(s) used to refine structure: *SHELXL2013* (Sheldrick, 2015); molecular graphics: *PLATON* (Spek, 2009); software used to prepare material for publication: *publCIF* (Westrip, 2010).

### 2-Oxo-2*H*-chromen-3-yl 4-chlorobenzoate

#### Crystal data

$C_{16}H_9ClO_4$   
 $M_r = 300.68$   
 Triclinic,  $P\bar{1}$   
 Hall symbol:  $-P\ 1$   
 $a = 6.7866$  (4) Å  
 $b = 7.1789$  (3) Å  
 $c = 14.0981$  (5) Å  
 $\alpha = 94.098$  (3)°  
 $\beta = 93.461$  (4)°  
 $\gamma = 106.154$  (4)°  
 $V = 655.75$  (5) Å<sup>3</sup>

$Z = 2$   
 $F(000) = 308$   
 $D_x = 1.523$  Mg m<sup>-3</sup>  
 Melting point: 478 K  
 Cu  $K\alpha$  radiation,  $\lambda = 1.54184$  Å  
 Cell parameters from 3886 reflections  
 $\theta = 6.3$ – $69.1$ °  
 $\mu = 2.72$  mm<sup>-1</sup>  
 $T = 293$  K  
 Prism, colourless  
 $0.12 \times 0.12 \times 0.08$  mm

#### Data collection

Agilent SuperNova Dual Source  
 diffractometer with an Atlas detector  
 Radiation source: fine-focus sealed tube  
 Graphite monochromator  
 Detector resolution: 5.3048 pixels mm<sup>-1</sup>  
 $\omega$  scan  
 Absorption correction: multi-scan  
 (*CrysAlis PRO*; Agilent, 2014)  
 $T_{\min} = 0.737$ ,  $T_{\max} = 0.812$

7634 measured reflections  
 2409 independent reflections  
 2109 reflections with  $I > 2\sigma(I)$   
 $R_{\text{int}} = 0.022$   
 $\theta_{\max} = 69.1$ °,  $\theta_{\min} = 6.3$ °  
 $h = -8 \rightarrow 7$   
 $k = -8 \rightarrow 8$   
 $l = -17 \rightarrow 16$

#### Refinement

Refinement on  $F^2$   
 Least-squares matrix: full  
 $R[F^2 > 2\sigma(F^2)] = 0.039$   
 $wR(F^2) = 0.106$   
 $S = 1.05$   
 2409 reflections  
 190 parameters

0 restraints  
 Primary atom site location: structure-invariant  
 direct methods  
 Secondary atom site location: difference Fourier  
 map  
 Hydrogen site location: inferred from  
 neighbouring sites

H-atom parameters constrained  
 $w = 1/[\sigma^2(F_o^2) + (0.0475P)^2 + 0.1948P]$   
 where  $P = (F_o^2 + 2F_c^2)/3$

$(\Delta/\sigma)_{\max} < 0.001$   
 $\Delta\rho_{\max} = 0.26 \text{ e } \text{\AA}^{-3}$   
 $\Delta\rho_{\min} = -0.49 \text{ e } \text{\AA}^{-3}$

### Special details

**Geometry.** All esds (except the esd in the dihedral angle between two l.s. planes) are estimated using the full covariance matrix. The cell esds are taken into account individually in the estimation of esds in distances, angles and torsion angles; correlations between esds in cell parameters are only used when they are defined by crystal symmetry. An approximate (isotropic) treatment of cell esds is used for estimating esds involving l.s. planes.

**Refinement.** Refinement of  $F^2$  against ALL reflections. The weighted R-factor wR and goodness of fit S are based on  $F^2$ , conventional R-factors R are based on F, with F set to zero for negative  $F^2$ . The threshold expression of  $F^2 > 2\text{sigma}(F^2)$  is used only for calculating R-factors(gt) etc. and is not relevant to the choice of reflections for refinement. R-factors based on  $F^2$  are statistically about twice as large as those based on F, and R-factors based on ALL data will be even larger.

### Fractional atomic coordinates and isotropic or equivalent isotropic displacement parameters ( $\text{\AA}^2$ )

	x	y	z	$U_{\text{iso}}^*/U_{\text{eq}}$
C1	0.1899 (3)	0.0796 (2)	0.35706 (12)	0.0446 (4)
C2	0.3804 (3)	0.0653 (2)	0.31891 (11)	0.0422 (4)
C3	0.5634 (3)	0.1322 (2)	0.36885 (11)	0.0414 (4)
H3	0.6815	0.1187	0.3424	0.050*
C4	0.5771 (2)	0.2250 (2)	0.46354 (11)	0.0384 (3)
C5	0.7616 (3)	0.3026 (2)	0.52035 (13)	0.0475 (4)
H5	0.8848	0.2943	0.4975	0.057*
C6	0.7618 (3)	0.3918 (3)	0.61044 (14)	0.0549 (5)
H6	0.8856	0.4451	0.6475	0.066*
C7	0.5794 (3)	0.4022 (3)	0.64594 (12)	0.0534 (5)
H7	0.5813	0.4628	0.7067	0.064*
C8	0.3938 (3)	0.3229 (2)	0.59161 (12)	0.0474 (4)
H8	0.2705	0.3270	0.6158	0.057*
C9	0.3956 (2)	0.2379 (2)	0.50103 (11)	0.0390 (3)
C10	0.3047 (3)	0.0312 (3)	0.15135 (12)	0.0459 (4)
C11	0.2730 (2)	-0.1155 (3)	0.06844 (12)	0.0458 (4)
C16	0.2973 (3)	-0.2994 (3)	0.07788 (13)	0.0525 (4)
H16	0.3335	-0.3326	0.1377	0.063*
C15	0.2683 (3)	-0.4333 (3)	-0.00072 (14)	0.0599 (5)
H15	0.2832	-0.5568	0.0058	0.072*
C14	0.2170 (3)	-0.3809 (4)	-0.08894 (14)	0.0626 (6)
C13	0.1904 (3)	-0.1999 (4)	-0.10068 (13)	0.0649 (6)
H13	0.1534	-0.1680	-0.1607	0.078*
C12	0.2200 (3)	-0.0667 (3)	-0.02135 (13)	0.0555 (5)
H12	0.2042	0.0564	-0.0282	0.067*
Cl1	0.18104 (10)	-0.55203 (13)	-0.18674 (4)	0.0951 (3)
O1	0.20802 (17)	0.16486 (17)	0.44814 (8)	0.0444 (3)
O2	0.0204 (2)	0.0211 (2)	0.31579 (10)	0.0637 (4)
O3	0.3603 (2)	-0.04346 (18)	0.23221 (8)	0.0516 (3)
O4	0.2900 (2)	0.1930 (2)	0.15125 (10)	0.0592 (3)

Atomic displacement parameters ( $\text{\AA}^2$ )

	$U^{11}$	$U^{22}$	$U^{33}$	$U^{12}$	$U^{13}$	$U^{23}$
C1	0.0428 (9)	0.0444 (8)	0.0465 (9)	0.0127 (7)	0.0018 (7)	0.0042 (7)
C2	0.0515 (10)	0.0402 (8)	0.0374 (8)	0.0177 (7)	0.0038 (7)	0.0026 (6)
C3	0.0424 (9)	0.0431 (8)	0.0433 (8)	0.0176 (7)	0.0101 (7)	0.0082 (7)
C4	0.0411 (8)	0.0336 (7)	0.0420 (8)	0.0117 (6)	0.0044 (6)	0.0066 (6)
C5	0.0426 (9)	0.0461 (9)	0.0549 (10)	0.0139 (7)	0.0001 (7)	0.0097 (7)
C6	0.0597 (11)	0.0467 (9)	0.0538 (10)	0.0117 (8)	-0.0144 (8)	0.0049 (8)
C7	0.0801 (13)	0.0438 (9)	0.0386 (8)	0.0230 (9)	-0.0015 (8)	0.0018 (7)
C8	0.0601 (11)	0.0458 (9)	0.0420 (8)	0.0230 (8)	0.0084 (7)	0.0057 (7)
C9	0.0417 (8)	0.0346 (7)	0.0428 (8)	0.0134 (6)	0.0045 (6)	0.0069 (6)
C10	0.0369 (9)	0.0587 (10)	0.0442 (9)	0.0156 (7)	0.0051 (7)	0.0082 (7)
C11	0.0341 (8)	0.0648 (11)	0.0388 (8)	0.0140 (7)	0.0044 (6)	0.0048 (7)
C16	0.0515 (10)	0.0651 (11)	0.0407 (9)	0.0181 (8)	0.0000 (7)	0.0006 (8)
C15	0.0541 (11)	0.0709 (12)	0.0519 (10)	0.0169 (9)	0.0015 (8)	-0.0073 (9)
C14	0.0401 (10)	0.0978 (16)	0.0434 (10)	0.0137 (10)	0.0043 (7)	-0.0134 (10)
C13	0.0437 (10)	0.1146 (19)	0.0370 (9)	0.0235 (11)	0.0029 (7)	0.0066 (10)
C12	0.0432 (10)	0.0826 (13)	0.0446 (9)	0.0217 (9)	0.0061 (7)	0.0141 (9)
C11	0.0754 (4)	0.1412 (6)	0.0550 (3)	0.0214 (4)	0.0009 (3)	-0.0395 (4)
O1	0.0383 (6)	0.0504 (6)	0.0464 (6)	0.0160 (5)	0.0069 (5)	0.0012 (5)
O2	0.0439 (7)	0.0792 (9)	0.0619 (8)	0.0120 (6)	-0.0056 (6)	-0.0029 (7)
O3	0.0686 (8)	0.0544 (7)	0.0369 (6)	0.0280 (6)	0.0000 (5)	-0.0007 (5)
O4	0.0689 (9)	0.0586 (8)	0.0561 (8)	0.0273 (7)	0.0046 (6)	0.0092 (6)

Geometric parameters ( $\text{\AA}$ ,  $^\circ$ )

C1—O2	1.206 (2)	C8—H8	0.9300
C1—O1	1.366 (2)	C9—O1	1.382 (2)
C1—C2	1.456 (2)	C10—O4	1.193 (2)
C2—C3	1.335 (2)	C10—O3	1.370 (2)
C2—O3	1.3809 (19)	C10—C11	1.479 (2)
C3—C4	1.435 (2)	C11—C16	1.390 (3)
C3—H3	0.9300	C11—C12	1.390 (2)
C4—C9	1.393 (2)	C16—C15	1.381 (3)
C4—C5	1.395 (2)	C16—H16	0.9300
C5—C6	1.380 (3)	C15—C14	1.377 (3)
C5—H5	0.9300	C15—H15	0.9300
C6—C7	1.382 (3)	C14—C13	1.381 (4)
C6—H6	0.9300	C14—C11	1.738 (2)
C7—C8	1.385 (3)	C13—C12	1.385 (3)
C7—H7	0.9300	C13—H13	0.9300
C8—C9	1.378 (2)	C12—H12	0.9300
O2—C1—O1	118.19 (16)	C8—C9—C4	122.08 (16)
O2—C1—C2	125.73 (17)	O1—C9—C4	120.91 (14)
O1—C1—C2	116.07 (14)	O4—C10—O3	122.83 (17)
C3—C2—O3	120.59 (15)	O4—C10—C11	127.29 (16)

---

C3—C2—C1	122.67 (15)	O3—C10—C11	109.86 (15)
O3—C2—C1	116.26 (15)	C16—C11—C12	119.31 (18)
C2—C3—C4	119.71 (15)	C16—C11—C10	121.73 (16)
C2—C3—H3	120.1	C12—C11—C10	118.96 (18)
C4—C3—H3	120.1	C15—C16—C11	120.64 (18)
C9—C4—C5	118.11 (15)	C15—C16—H16	119.7
C9—C4—C3	118.07 (15)	C11—C16—H16	119.7
C5—C4—C3	123.81 (15)	C14—C15—C16	118.9 (2)
C6—C5—C4	120.22 (17)	C14—C15—H15	120.5
C6—C5—H5	119.9	C16—C15—H15	120.5
C4—C5—H5	119.9	C15—C14—C13	121.89 (19)
C5—C6—C7	120.47 (17)	C15—C14—C11	118.0 (2)
C5—C6—H6	119.8	C13—C14—C11	120.05 (16)
C7—C6—H6	119.8	C14—C13—C12	118.72 (18)
C6—C7—C8	120.40 (17)	C14—C13—H13	120.6
C6—C7—H7	119.8	C12—C13—H13	120.6
C8—C7—H7	119.8	C13—C12—C11	120.5 (2)
C9—C8—C7	118.70 (17)	C13—C12—H12	119.7
C9—C8—H8	120.6	C11—C12—H12	119.7
C7—C8—H8	120.6	C1—O1—C9	122.54 (13)
C8—C9—O1	117.01 (15)	C10—O3—C2	118.78 (14)
O2—C1—C2—C3	-179.51 (17)	O4—C10—C11—C12	0.0 (3)
O1—C1—C2—C3	-0.5 (2)	O3—C10—C11—C12	-178.60 (15)
O2—C1—C2—O3	-7.4 (3)	C12—C11—C16—C15	-0.3 (3)
O1—C1—C2—O3	171.59 (13)	C10—C11—C16—C15	-179.53 (16)
O3—C2—C3—C4	-172.69 (13)	C11—C16—C15—C14	0.7 (3)
C1—C2—C3—C4	-0.9 (2)	C16—C15—C14—C13	-1.1 (3)
C2—C3—C4—C9	1.5 (2)	C16—C15—C14—C11	-179.94 (15)
C2—C3—C4—C5	-178.72 (15)	C15—C14—C13—C12	1.1 (3)
C9—C4—C5—C6	-1.0 (2)	C11—C14—C13—C12	179.94 (14)
C3—C4—C5—C6	179.23 (15)	C14—C13—C12—C11	-0.7 (3)
C4—C5—C6—C7	1.1 (3)	C16—C11—C12—C13	0.3 (3)
C5—C6—C7—C8	0.2 (3)	C10—C11—C12—C13	179.57 (16)
C6—C7—C8—C9	-1.5 (3)	O2—C1—O1—C9	-179.48 (15)
C7—C8—C9—O1	-178.39 (14)	C2—C1—O1—C9	1.4 (2)
C7—C8—C9—C4	1.6 (2)	C8—C9—O1—C1	179.09 (14)
C5—C4—C9—C8	-0.4 (2)	C4—C9—O1—C1	-0.9 (2)
C3—C4—C9—C8	179.42 (14)	O4—C10—O3—C2	6.6 (3)
C5—C4—C9—O1	179.60 (13)	C11—C10—O3—C2	-174.68 (14)
C3—C4—C9—O1	-0.6 (2)	C3—C2—O3—C10	-115.15 (18)
O4—C10—C11—C16	179.25 (18)	C1—C2—O3—C10	72.60 (19)
O3—C10—C11—C16	0.6 (2)		

---